

phonon renormalization parameter.

Using an empirically fitted three-OPW band model, prediction of the resonance fields due to electrons at the lens rim in a (0001) sample yielded fields 10% lower than those observed experimentally. This may perhaps be explained by the insufficient number of plane waves or by the fact that the pseudopotentials used were local.

An attempt to predict the resonance field anisotropy for the complex second-band "monster" yielded qualitative agreement with experiment. We believe that nonlocal pseudopotential band descriptions would yield considerably better agreement with experiment, and would allow extraction of the electron-phonon renormalization parameter at points on the monster.

*Work supported by an NSF University Science Development Grant.

¹M. S. Khaikin, Zh. Eksperim. i Teor. Fiz. **39**, 212 (1960) [Sov. Phys. JETP **12**, 152 (1961)].

²J. F. Koch and C. C. Kuo, Phys. Rev. **143**, 470 (1966).

³R. E. Prange and T. W. Nee, Phys. Rev. **168**, 779 (1968).

⁴T. W. Nee, J. F. Koch, and R. E. Prange, Phys. Rev. **174**, 758 (1968).

⁵J. F. Koch and J. D. Jensen, Phys. Rev. **184**, 643 (1969).

⁶J. F. Koch and T. E. Murray, Phys. Rev. **186**, 722 (1969).

⁷J. F. Koch and R. E. Doezema, Phys. Rev. Letters **24**, 507 (1970).

⁸A. F. Kip, D. N. Langenberg, and T. W. Moore, Phys. Rev. **124**, 359 (1961).

⁹J. J. Sabo, Jr., Phys. Rev. B **1**, 1479 (1970).

¹⁰W. J. McG. Tegart, *The Electrolytic and Chemical Polishing of Metals* (Pergamon, New York, 1959).

¹¹R. E. Doezema and J. F. Koch, Phys. Rev. B **5**, 3866 (1972).

¹²M. P. Shaw, T. G. Eck, and D. A. Zych, Phys. Rev. **142**, 406 (1966).

¹³R. C. Jones, R. G. Goodrich, and L. M. Falicov, Phys. Rev. **174**, 672 (1968).

¹⁴M. J. G. Lee, Phys. Rev. B **2**, 250 (1970).

Magnetic Field Dependence of the Ultrasonic Attenuation of Shear Waves in Cesium*

B. Keramidias,[†] J. Trivisonno, and G. Kaltenbach

Department of Physics, John Carroll University, Cleveland, Ohio 44118

(Received 26 June 1972)

The magnetic field dependence of the ultrasonic attenuation of shear waves has been measured in high-purity single crystals of cesium. Measurements were made at frequencies between 15 and 87 MHz at 4.2 and 1.3 °K, corresponding to a range in ql from 1 to 35. The results are compared with the Cohen-Harrison-Harrison theory of ultrasonic attenuation and with previous studies done on potassium. The results agree rather well with theory and the discrepancies that are observed are similar to those observed in potassium.

I. INTRODUCTION

A large number of ultrasonic-attenuation experiments¹⁻⁷ have been conducted to test the free-electron theories⁸⁻¹⁰ of ultrasonic attenuation due to conduction electrons. Potassium, which has a Fermi surface that is very nearly spherical, has been the subject of most of these studies. While most of the experimental results have been in agreement with theory, discrepancies have been reported⁷ in the high-field attenuation of longitudinal waves in a transverse magnetic field. Blaney⁶ has also reported some departures from theory at high ql values in the attenuation of shear waves in a transverse field.

Cesium is an ideal metal to study the effect of a Fermi surface which is slightly distorted from a spherical shape on the predictions of the free-electron

theory of the ultrasonic attenuation due to conduction electrons. The Fermi surface of cesium bulges in the [110] direction by about 5% and is depressed in the [100] and [111] directions by 1 and 1.2%, respectively. The radial anisotropy was first deduced from de Haas-van Alphen data by Okumura and Templeton¹¹ and later directly measured in this laboratory using the magnetoacoustic effect with longitudinal waves.¹²

The present investigation deals with the magnetic field dependence of ultrasonic attenuation of shear waves in single crystals of cesium. For shear waves propagating in a transverse magnetic field, the Cohen-Harrison-Harrison theory (CHH)⁹ predicts the magnetic field dependence both for the case of shear waves polarized perpendicular to the field and for waves polarized parallel to the field. When \vec{H} is perpendicular to \vec{P} and $ql > 3$, the atten-

uation is oscillatory for $qR \geq 4$ and goes to zero as qR approaches 0. The wave number is q , l is the electron mean free path, and $R = \hbar k_F c / eH$ is the radius of the orbit on the Fermi surface. The extrema occur whenever $qR = (n + \gamma)\pi$, where n is an integer for maxima and half-odd integer for minima and γ is the phase factor given by the theory. The oscillations are periodic in $1/H$, and \vec{k}_F is the Fermi wave vector. When the magnetic field is parallel to the polarization of the wave, the attenuation decreases monotonically with the field and approaches zero as qR goes to zero. The total change in the attenuation is then a measure of the absolute electronic contribution to the attenuation.

In comparing the experimental results, the expressions derived by Flax and Trivisonno¹³ from the CHH theory are used. These expressions are valid for all ql values and reduce to Pippard's¹⁴ results in zero field.

II. EXPERIMENTAL PROCEDURE

The techniques for growing and orienting the cesium crystals have been described in previous publications.^{12,15} The orientation of a crystal boule was done optically to obtain the nearest [110] or [100] direction. An x ray of a thin slice was taken to check the orientation and to determine the proper polarization direction. It is extremely difficult to orient the final acoustic specimens better than 3° or 4° so that in material as highly anisotropic as cesium the shear waves in some cases are quasi-shear-waves.

ac-cut 5-MHz transducers were used to transmit and receive the signals. The ultrasonic system and automatic recording of signal amplitude vs magnetic field have also been described in previous publications.^{12,16} Measurements were made on four single crystals. Numerous runs were attempted on other crystals but for various experimental reasons such as broken bonds, poor sample purity, and misalignment of the shear transducers, little or no data were obtained. The data that are presented in Sec. III were obtained on two crystals.

Crystal 1 had a length of 0.42 cm and was oriented along [110] and the polarization of the shear transducer was along [001] which corresponds to the shear wave associated with the elastic constant C_{44} . The velocity of the wave was 0.89×10^5 cm/sec. This velocity was measured at 5 MHz and agrees with the value obtained in a previous study of the elastic constants of cesium.¹⁵ Ultrasonic frequencies between 15 and 85 MHz were employed and measurements were taken at 4.2 and 1.3 °K. The echoes obtained in this particular run were extremely good and for frequencies as high as 75 MHz were noise free. In addition, as the field was rotated on either side of the [001] direction, the direction of \vec{P} , symmetrical-attenuation-vs-field

plots were obtained. Crystal 2 was oriented along [001] and the polarization was along [110]. For propagation along [001] the shear waves are degenerate and the velocity corresponding to the elastic constant C_{44} is obtained independent of the direction of polarization of the wave. The crystal length was 0.38 cm and the sound velocity was 0.85×10^5 cm/sec. This crystal was approximately 5° off from [001] and the poor symmetry of the attenuation plots indicates that \vec{P} was also not along the [110] symmetry direction. Ultrasonic frequencies between 15 and 55 MHz were studied. The other two crystals for which data were obtained were for $\vec{q} \parallel [110]$ and $\vec{q} \parallel [100]$ with $\vec{p} \parallel [001]$ in both cases. For the [110] crystal, only low-frequency data were obtained and agree with the data reported for crystal 1. For the [001] crystal, the cesium acoustic specimen spontaneously ignited when the sample was being removed from the ultrasonic probe and no accurate measurement of the length was obtained. Those data which could be analyzed in a relative manner such as the frequency dependence were in agreement with the results reported in Sec. III for crystals 1 and 2.

III. RESULTS AND DISCUSSION

Typical plots of echo amplitude versus magnetic field are shown in Figs. 1 and 2 for ultrasonic frequencies of 55 and 85 MHz. These curves are tracings of the actual x - y recorder plots for data taken on crystal 1. In all cases, the magnetic field is along [110] and is perpendicular to the direction of propagation and the polarization of the wave. The upper curve shown in each figure is for a temperature of 4.2 °K and the lower curve for data taken at 1.3 °K. The electron mean free path is phonon limited at 4.2 °K and becomes impurity limited at 1.3 °K. Residual-resistance experiments on similar samples using an eddy-current technique indicated that the electron mean free path

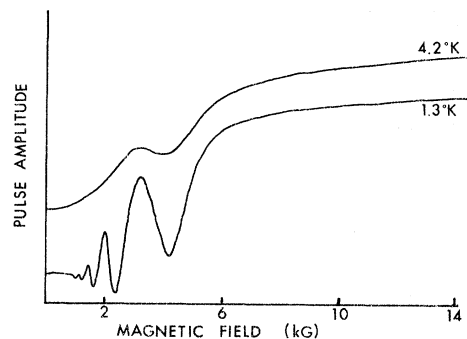


FIG. 1. Variation of echo amplitude with magnetic field for an ultrasonic frequency of 55 MHz. \vec{H} is perpendicular to \vec{q} and \vec{P} .

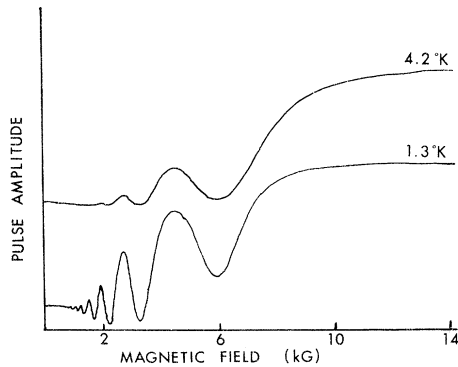


FIG. 2. Variation of echo amplitude with magnetic field for an ultrasonic frequency of 85 MHz.

increases by a factor of 4–6 between 4.2 and 1.3 °K. These two figures then illustrate both the effect of ultrasonic frequency and electron mean free path on the magnetic field dependence of the ultrasonic attenuation. For either temperature the attenuation is qualitatively in agreement with the free-electron theory and the results of similar experiments done on potassium. That is, the oscillations become more numerous and stronger as the frequency and mean free path increase and the attenuation decreases and saturates at high fields.

The effect of varying the angle between the magnetic field direction and the polarization of the shear wave is shown in Fig. 3 as H is rotated in the (110) plane which is perpendicular to the direction of propagation. The frequency is 87 MHz and the temperature is 1.3 °K. The bottom curve corresponds to \vec{H} perpendicular to \vec{P} which is along the [001] direction. The angle between \vec{H} and \vec{P} is 45° for the middle curve and the top curve is for \vec{H}

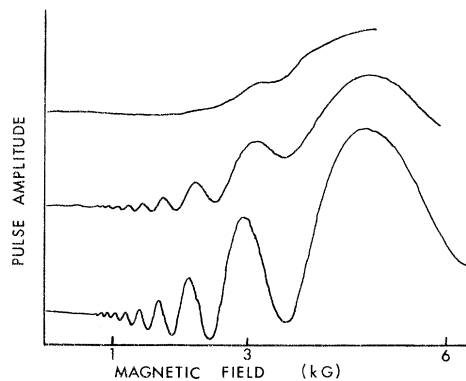


FIG. 3. Dependence of the relative attenuation with magnetic field for various orientations of \vec{H} relative to \vec{P} . For all curves, \vec{H} is perpendicular to \vec{q} . For the upper curve, \vec{H} is parallel to \vec{P} , for the middle curve \vec{H} is at an angle of 45° with respect to \vec{P} , and in the lower curve \vec{H} is perpendicular to \vec{P} .

parallel to \vec{P} . The curves are at least in qualitative agreement with the free-electron theory which predicts that the attenuation is nonoscillatory when \vec{H} is parallel to \vec{P} . For \vec{H} perpendicular to \vec{P} , 29 easily discernible extrema were obtained at 87 MHz. The plot of extrema versus $1/H$ was extremely linear. The slope of this plot yields the period of the oscillations and is used to obtain the Fermi momentum. The momentum corresponding to the direction $\vec{q} \times \vec{H}$ measured in this case is in the [001] direction or the direction of \vec{P} . The value obtained of 6.93×10^{-20} g cm/sec agrees quite well with the free-electron value of 6.83×10^{-20} g cm/sec. A value 1% lower than the free-electron value is expected in this direction. The measured momentum depends on the accuracy with which one can measure the period of the oscillations, the ultrasonic frequency, and the sound velocity. In cesium, values better than 3% are difficult to obtain. Unlike the case with longitudinal waves where the radial anisotropy can be determined by measuring the change in the period of oscillation as H is rotated in a plane perpendicular to \vec{q} , only an absolute momentum can be obtained with shear waves. In a

TABLE I. Comparison of experimental and theoretical values of qR for attenuation extrema.

| Extremum number n | qR Theory | $qR_{\text{ext}} = 2\pi cp / \lambda eH$ | |
|------------------------|----------------|--|--------|
| | | 85 MHz | 55 MHz |
| 1 | 4.2 | 4.6 | ... |
| 2 | 7.4 | 7.4 | 7.3 |
| 3 | 10.6 | 10.8 | 10.4 |
| 4 | 13.6 | 14.1 | 13.6 |
| 5 | 16.9 | 17.3 | 16.7 |
| 6 | 20.0 | 20.4 | 19.8 |
| 7 | 23.1 | 23.4 | 23.0 |
| 8 | 26.3 | 26.3 | ... |
| 9 | 29.4 | 29.5 | ... |
| 10 | 32.5 | 32.9 | ... |
| $\frac{3}{2}$ | 5.6 | 6.2 | ... |
| $\frac{5}{2}$ | 8.8 | 9.0 | 8.6 |
| $\frac{7}{2}$ | 12.0 | 12.4 | 11.9 |
| $\frac{9}{2}$ | 15.3 | 15.6 | 15.1 |
| $\frac{11}{2}$ | 18.4 | 18.8 | 18.3 |
| $\frac{13}{2}$ | 21.6 | 21.9 | 21.4 |
| $\frac{15}{2}$ | 24.7 | 25.0 | ... |
| $\frac{17}{2}$ | 27.8 | 28.3 | ... |
| $\frac{19}{2}$ | 31.0 | 31.3 | ... |
| $\frac{21}{2}$ | 34.0 | ... | ... |

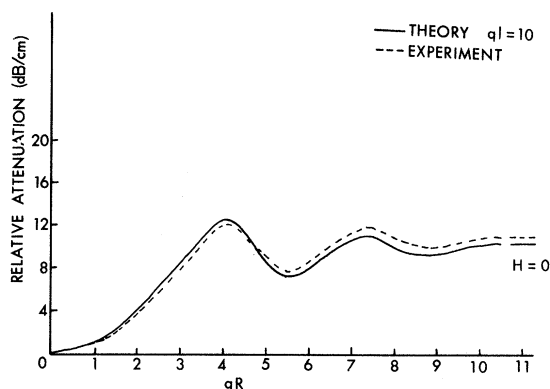


FIG. 4. Relative attenuation in dB/cm vs qR for a frequency of 25 MHz. The corresponding theoretical curve for a ql of 10 is also shown. The attenuation is measured relative to the high-field attenuation.

given experiment only one caliper can be obtained unambiguously. The present experiment is therefore concerned with a detailed comparison of the attenuation curves with the predictions of the free-electron theory and the effect of a slightly anisotropic Fermi surface on these results.

One means of comparison is to examine the positions of the attenuation extrema. This comparison between experiment and free-electron theory is given in Table I for 55 and 87 MHz. The theoretical values of qR were taken from CHH theory since for these frequencies we estimated ql greater than 20. Flax and Trivisonno¹³ have shown that the first few maxima are slightly ql dependent and shift to large qR values as ql increases, but are essentially independent of ql for ql greater than 20. For n an integer, maxima in the attenuation occur, and for n a half-odd integer, minima in the attenuation occur. The experimental values for the frequencies shown were calculated from the mea-

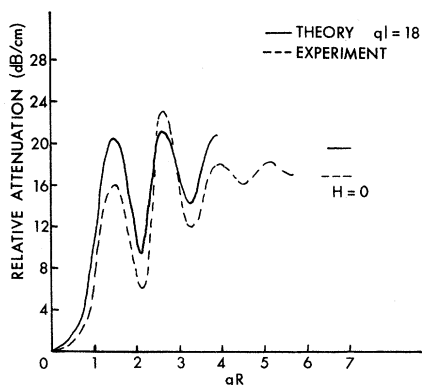


FIG. 5. Relative attenuation in dB/cm vs qR for a frequency of 45 MHz.

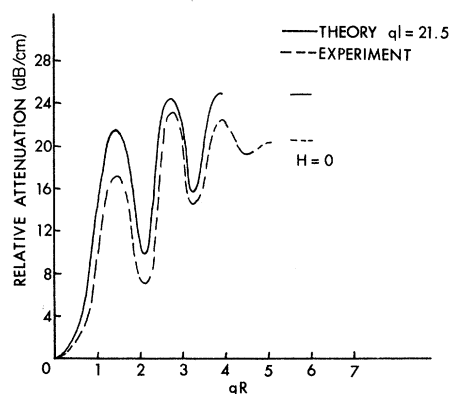


FIG. 6. Relative attenuation in dB/cm vs qR for a frequency of 54.5 MHz.

sured period of the oscillations and the field value at which the extrema occurred. The value of the quantities is accurate to about 3%. With the exception of the first two extrema, which occur at high fields, the agreement between theory and experiment is excellent.

Since the ordinates of the x - y plots were calibrated directly in dB, the entire experimental attenuation curves may be compared with the theoretical curves. In Fig. 4, the attenuation in dB/cm relative to the high-field attenuation is plotted vs $1/H\lambda$ for a frequency of 25 MHz. The corresponding theoretical curve shown is for $ql=10$. The total change in attenuation is in good agreement with theory. While the oscillation strengths are strongly dependent on ql , the total attenuation is not a very strong function of ql for ql greater than 5. The theoretical curves for $ql=9$ and 11 give essentially the same total change, but the oscillations for the $ql=10$ curve give better agreement with experiment. In addition, at 15 MHz the attenuation is still oscillatory so that ql is around 5 or 6 indicating that a ql value of 10 at 25 MHz is reasonable.

In Fig. 5 a similar plot is shown for a frequency of 45 MHz and a theory curve corresponding to $ql=18$. The total change in attenuation observed is less than the theoretical value which is now essentially independent of the choice of ql . In Figs. 6 and 7 similar comparisons are made for frequencies; the total change in the measured attenuation is less than that predicted by theory and the difference is larger as the frequency increases.

When \vec{H} is parallel to \vec{P} , the attenuation essentially decreases monotonically with increasing H and at the lower frequencies saturates at the same value as for the case of \vec{H} perpendicular to \vec{P} . At the higher frequencies, the attenuation saturates at a lower value for \vec{H} parallel to \vec{P} . The theory predicts that $\alpha(H)$ approaches 0 as $1/H^2$ indepen-

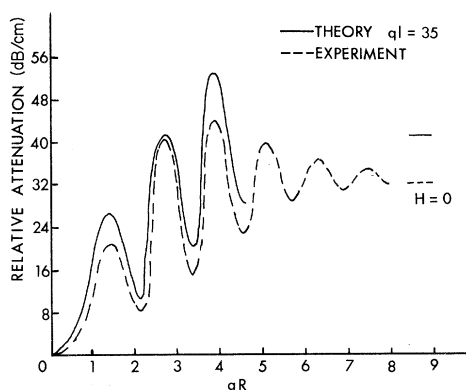


FIG. 7. Relative attenuation in dB/cm vs qR for a frequency of 87 MHz.

dent of the angle between \vec{H} and \vec{P} , and thus the total change between zero field and infinite field should be a measure of the electronic contribution to the attenuation at zero field. The experimental data fall off as $1/H^2$ and at the lower frequencies are saturated at 14 kG. For \vec{H} perpendicular to \vec{P} , the attenuation is saturated at all frequencies for data at 1.3 °K and 14 kG. For \vec{H} parallel to \vec{P} , the attenuation reaches a saturation value more slowly. Unfortunately we did not make a full field sweep for this geometry at 87 or 77 MHz where a sizable anisotropy was observed at 14 kG and thus we were not able to extrapolate the data to infinite field. The extrapolated data at 65 MHz do indicate, however, that anisotropy is in fact present. The attenuation listed for $\vec{H} \parallel \vec{P}$ for frequencies of 77 and 87 MHz is slightly higher than shown in Table II for reasons discussed above. The results summarized in Table II are for frequencies from 15 to 87 MHz. The corresponding theoretical values are also listed, and the theory predicts the same attenuation change for $\vec{H} \parallel \vec{P}$ and $\vec{H} \perp \vec{P}$. The experimental values have an absolute accuracy of 5–10%. The relative accuracy is known much more accurately. The theoretical values are uncertain to about 4% since the scaling factor used to calculate the attenuation contains the sound velocity and ultrasonic frequency. The over-all agreement with theory is

TABLE II. Comparison of observed attenuation changes between zero field and 14 kG with the corresponding theoretical values. Crystal 1: $\vec{q} \parallel [011]$ and $\vec{P} \parallel [100]$.

| Frequency | $\Delta\alpha$ (dB/cm) $\vec{H} \parallel \vec{P}$ | Experimental $\vec{H} \perp \vec{P}$ | $\Delta\alpha$ (dB/cm) theory | ql |
|-----------|---|---|----------------------------------|------|
| 15 | 7.4 | 7.4 | 5.8 | 6 |
| 25 | 11.4 | 11.4 | 10.2 | 10 |
| 45 | 17.8 | 17.8 | 19.4 | 18 |
| 55 | 20.7 | 21.4 | 24.5 | 21.5 |
| 66 | 23.5 | 25.0 | 29.3 | 26.5 |
| 77 | 21.2 | 22.6 | 34.4 | 30.5 |
| 87 | 31.5 | 34.0 | 39.0 | 35 |

therefore fairly good, but the nonlinear frequency dependence represents a departure from theory.

While the amplitude of the oscillations shown in Figs. 4–7 agrees within experimental error with theory, the background attenuation is different, which affects the high-field oscillations more strongly than the low-field oscillations. In particular, at high ql values the amplitudes of attenuation minima oscillate above the zero-field value while the corresponding theoretical minima are below the zero-field value. This is most clearly seen by arbitrarily displacing the experimental curve upward so that the zero-field attenuations coincide. While the theory curves shown were calculated for arbitrary ql values, we did assume $\omega\tau \ll 1$ or $(V_s/V_p)ql \ll 1$. Since the sound velocity V_s is much lower in cesium than in a typical metal, $\omega\tau$ is about $\frac{1}{20}$ for $ql = 35$ so that this condition is reasonably satisfied.

We also made measurements on a second crystal oriented along the [001] direction. The transducer was placed on the crystal so that the polarization was along [110]. This orientation was chosen so that when \vec{H} is perpendicular to \vec{P} and along the $[1\bar{1}0]$ direction, the caliper associated with momentum in the [110] direction in k space is obtained and it is in this direction that the Fermi surface bulges by about 5%. In our previous study using longitudinal wave with $\vec{q} \parallel [001]$ and $\vec{H} \parallel [110]$ directions, the high-field oscillations were washed out. The amplitude of the geometric oscillations of the shear waves, however, was essentially the same as for crystal 1. The momentum determined from the period of these oscillations had a value of 6.91×10^{-20} g cm/sec. A value of 7.1×10^{-20} g cm/sec is expected for this geometry but misorientation effects and the accuracy to which the frequency and sound velocity are known can easily account for this difference. The positions of the attenuation extrema were in agreement with theory. Again, however, the attenuation did not scale linearly with frequency and at higher frequencies the measured attenuation is significantly less than theory. These results are shown in Table III. The agreement with theory is not as good as for crystal 1 at low frequencies and may be associated with misorientation effects or crystal-length

TABLE III. Comparison of observed attenuation changes between zero field and 14 kG with the corresponding theoretical values. Crystal 2: $\vec{q} \parallel [001]$ and $\vec{P} \parallel [110]$.

| Frequency | $\Delta\alpha$ ($\vec{H} \perp \vec{P}$) | $\Delta\alpha$ (theory) | ql |
|-----------|--|-------------------------|------|
| 15 | 8.4 | 5.9 | 6 |
| 25 | 14.9 | 10.6 | 10 |
| 35 | 17.5 | 15.3 | 14 |
| 55 | 17.5 | 24.9 | 21.5 |

determination. Nevertheless, the nonlinear frequency dependence observed is independent of the length and sound velocity, and for free electrons should be independent of the angle between \vec{H} and \vec{P} .

The small departures (lower attenuation) observed at higher frequencies could be attributed to the distortions in Fermi surface. The maximum distortion of the Fermi surface in cesium is 6%. At high ql values a very narrow belt of electrons on the surface contributes to the attenuation and it is very reasonable that the discrepancies discussed above can be attributed to the small distortions on the Fermi surface. This feature alone, however, cannot explain the nonlinear frequency dependence that was observed. While the free-electron theory predicts $\alpha(H)$ goes to zero at high fields for shear waves, as does the real-metal theory of Pippard,¹⁰ other investigators^{16,17} studying more complicated metals have observed that $\alpha(H)$ does not vanish at high fields. If the attenuation

does not vanish at high fields but approaches some finite value which is a function of ql , then the nonlinear frequency dependence and the anisotropy can be explained. Blaney⁶ has reported similar departures from theory in potassium at high ql values despite the very nearly spherical Fermi surface of potassium.

In summary, with the exception of the discrepancies observed at high ql values, the magnetic field dependence of the ultrasonic attenuation of shear waves is in rather good agreement with the free-electron theory. The departures that are observed are similar to those obtained in potassium and are most likely explained by a nonvanishing of the attenuation at high fields. These results are somewhat surprising since in our study of longitudinal waves rather large departures from theory were observed. A more detailed study of longitudinal waves will be the subject of a future publication.

*Work supported in part by AFOSR and NSF under Grant No. GH-31652.

†Presently at Pennsylvania State University.

¹H. J. Foster, P. Meijer, and V. Mielczarek, *Phys. Rev.* **139**, A1849 (1965).

²J. Trivisonno, M. S. Said, and L. A. Pauer, *Phys. Rev.* **147**, 518 (1966).

³M. S. Said, J. C. Worley, and J. Trivisonno, *Phys. Letters* **21**, 280 (1966).

⁴R. L. Thomas and H. V. Bohm, *Phys. Rev. Letters* **16**, 587 (1966).

⁵M. P. Greene, A. R. Hoffman, A. Houghton, and J. J. Quinn, *Phys. Rev.* **156**, 798 (1967).

⁶T. G. Blaney, *Phil. Mag.* **17**, 405 (1968).

⁷J. R. Peverley, *Phys. Rev.* **173**, 689 (1968).

⁸T. Kjeldaas and T. Holstein, *Phys. Rev. Letters* **2**, 340 (1959).

⁹M. H. Cohen, M. J. Harrison, and W. A. Harrison, *Phys. Rev.* **117**, 937 (1960).

¹⁰A. B. Pippard, *Proc. Roy. Soc. (London)* **A257**, 165 (1960).

¹¹K. Okumura and J. M. Templeton, *Phil. Mag.* **8**, 89 (1963).

¹²J. Trivisonno and J. A. Murphy, *Phys. Rev. B* **1**, 3341 (1970).

¹³L. Flax and J. Trivisonno, *Phys. Letters* **22**, 280 (1960).

¹⁴A. B. Pippard, *Phil. Mag.* **46**, 1104 (1955).

¹⁵F. J. Kollaritis and J. Trivisonno, *J. Phys. Chem. Solids* **29**, 2133 (1968).

¹⁶R. V. Kollaritis, J. Trivisonno, and R. W. Stark, *Phys. Rev. B* **2**, 1508 (1970).

¹⁷B. K. Jones, *Phil. Mag.* **9**, 217 (1964).